brightness seems to be diminishing slowly. Still unknown are the approximate birthday of this strange supernova, its maximum luminosity, and its relationship (if any) to remnants such as Cas A.

We thank J. Carrasco, J. Henning, and D. Tennant for assistance at Palomar Observatory. A photograph confirming the presence of the supernova was obtained by E. A. Harlan with the 0.9-m Crossley telescope at Lick Observatory. R. A. Sramek provided radio data from the Very Large Array in Socorro, New Mexico. Informative discussions with K. Ebneter, J. L. Greenstein, C. F. McKee, and J. B. Oke are appreciated. This work was supported by the Miller Institute for Basic Research in Science (University of California at Berkeley) and by NSF grant AST 82-16544.

Received 19 March; accepted 10 June 1985.

1. Filippenko, A. V. & Sargent, W. L. W. *Astrophys. J. Suppl.* **57**, 503-522 (1985).
2. Filippenko, A. V. & Sargent, W. L. W. *IAU Circ.* No. 4042 (1985).
3. Sandage, A. & Tammann, G. A. *A Revised Shapley-Ames Catalog of Bright Galaxies* (Carnegie Institution of Washington, 1981).
4. Oke, J. B. & Gunn, J. E. *Publ. astr. Soc. Pacif.* **94**, 586-594 (1982).
5. Oke, J. B. & Gunn, J. E. *Astrophys. J.* **266**, 713-717 (1983).
6. Filippenko, A. V. *Publ. astr. Soc. Pacif.* **94**, 715-721 (1982).
7. Cantó, J., Elliott, K. H., Meaburn, J. & Theokas, A. C. *Mon. Not. R. astr. Soc.* **193**, 911-919 (1980).
8. Brocklehurst, M. *Mon. Not. R. astr. Soc.* **153**, 471-490 (1971).
9. Huchra, J. *et al. Astr. J.* **90**, 691-696 (1985).
10. Humason, M. L., Mayall, N. U. & Sandage, A. R. *Astr. J.* **61**, 97-162 (1956).
11. Vaucouleurs, A. de & Vaucouleurs, G. de *Astr. J.* **72**, 730-737 (1967).
12. Filippenko, A. V. & Sargent, W. L. W. *IAU Circ.* No. 4048 (1985).
13. Gibson, J. & Schombert, J. *IAU Circ.* No. 4048 (1985).
14. Merrill, P. W. *Lines of the Chemical Elements in Astronomical Spectra* (Carnegie Institution of Washington, 1958).
15. Minkowski, R. *Astrophys. J.* **89**, 156-217 (1939).
16. Kirshner, R. P., Oke, J. B., Penston, M. V. & Searle, L. *Astrophys. J.* **185**, 303-322 (1973).
17. Kirshner, R. P. & Oke, J. B. *Astrophys. J.* **200**, 574-581 (1975).
18. Branch, D. *et al. Astrophys. J.* **270**, 123-139 (1983).
19. Oke, J. B. & Searle, L. *A. Rev. Astr. Astrophys.* **12**, 315-329 (1974).
20. Branch, D. *et al. Astrophys. J.* **244**, 780-804 (1981).
21. Niemela, V. S., Ruíz, M. T. & Phillips, M. M. *Astrophys. J.* **289**, 52-57 (1985).
22. Zwicky, F. in *Stars and Stellar Systems*, Vol. 8 (eds Aller, L. H. & McLaughlin, D. B.) 367-423 (University of Chicago Press, 1965).
23. Greenstein, J. L. & Minkowski, R. *Astrophys. J.* **182**, 225-243 (1973).
24. Tammann, G. A. in *Proc. NATO Advanced Study Institute on Supernovae* (eds Rees, M. J. & Stoneham, R. J.) 371-403 (Reidel, Dordrecht, 1981).
25. Shklovsky, I. S. *Supernovae* (Wiley, London, 1968).
26. Kirshner, R. P. & Chevalier, R. A. *Astrophys. J.* **218**, 142-147 (1977).
27. Chevalier, R. A. & Kirshner, R. P. *Astrophys. J.* **233**, 154-162 (1979).
28. Lasker, B. M. *Astrophys. J.* **223**, 109-121 (1978).
29. Balick, B. & Heckman, T. *Astrophys. J. Lett.* **226**, L7-L10 (1978).
30. Kirshner, R. P. & Blair, W. P. *Astrophys. J.* **236**, 135-142 (1980).
31. Chevalier, R. A. *Astrophys. J.* **208**, 826-828 (1976).
32. Wenzel, W. *IAU Circ.* No. 4049 (1985).
33. Filippenko, A. V. & Sargent, W. L. W. *Astr. J.* (submitted).

Molecular events during maturation of the immune response to oxazolone

C. Berek, G. M. Griffiths* & C. Milstein

Medical Research Council Laboratory of Molecular Biology, Hills Road, Cambridge CB2 2QH, UK

Sequence analysis of the heavy- and light-chain messenger RNA of hybridomas immunized with a specific hapten yields important clues about the interplay between genetic and selective events during the onset and maturation of the immune response. The maturation of the primary response to the hapten 2-phenyl-5-oxazolone is characterized by a drift to higher-affinity somatic variants of a germline-encoded basic sequence, whereas hybridomas from the secondary response demonstrate a further maturation dominated by a shift to alternative germline combinations.

THERE are good reasons to believe that drastic changes occur during the maturation[1] of an immune response and that primary- and secondary-response antibodies produced to the same antigen are structurally very different. The early stages of a response to an antigenic stimulus are often of a restricted nature[2-4], and followed by a change to an apparently more diverse response correlated with an increase in affinity for the antigen. The primary antibodies to (4-hydroxy-3-nitrophenyl)acetyl (NP) have λ chains and are heteroclitic, whereas the hyperimmune antibodies have κ chains, are no longer heteroclitic and show a high affinity for the immunizing antigen[5,6]. Similarly, antibodies to phosphorylcholine coupled to keyhole limpet haemocyanin (KLH) from the primary and secondary responses have different structures as well as increased affinity[7,8]. However, the difference in fine specificity suggests that the structural changes are probably associated with a change in hapten presentation (cell wall of microorganisms and KLH).

More extensive structural information is essential to elucidate the mechanism of known genetic processes that generate antibody diversity (reviewed in ref. 9) in response to a single antigenic stimulant. Antibody diversity arises in several ways: (1) germline diversity resulting from the multiple copies of variable (V), diversity (D) and joining (J) segments; (2) combinatorial diversity resulting from the use of alternative combinations of these genes; (3) junctional diversity resulting from variations in the joining of the gene segments; (4) somatic point mutations throughout the V regions. How do these mechanisms contribute to the maturation of an immune response?

To study this question, we have isolated hybridomas generated at three stages of the immune response to the hapten 2-phenyl-5-oxazolone (phOx) and determined the sequence of the messenger RNA for the corresponding antibody heavy (H) and light (L) chains. The response at day 7 was found to be restricted. Most of the antibody-secreting cells expressed a H/L chain combination encoded by a pair of germline genes, V_H-*Ox1* and V_κ-*Ox1*, respectively[10]. One week later (14 days after the primary injection) most antibodies still expressed similar, but no longer identical, sequences, suggesting a high degree of somatic mutation[11]. These changes were associated with an increase in affinity for the hapten.

Here, we report the analysis of the secondary response. We were surprised to find that the germline gene combination and variants that characterized the primary response constitute only a minor fraction of the phOx-specific hybridoma lines. The sequences demonstrate that what characterizes the secondary response is the dominant role of new germline H/L-chain gene combinations. We suggest that, although somatic mutation is a major factor in the genetic drift towards better antibodies characteristic of the maturation of the immune response to phOx, the shift towards alternative germline gene expression is equally important in the strategy for obtaining further improvements in antibody affinity at later stages of the response.

* Present address: Department of Pathology, Stanford University Medical Center, Stanford, California 94305, USA.

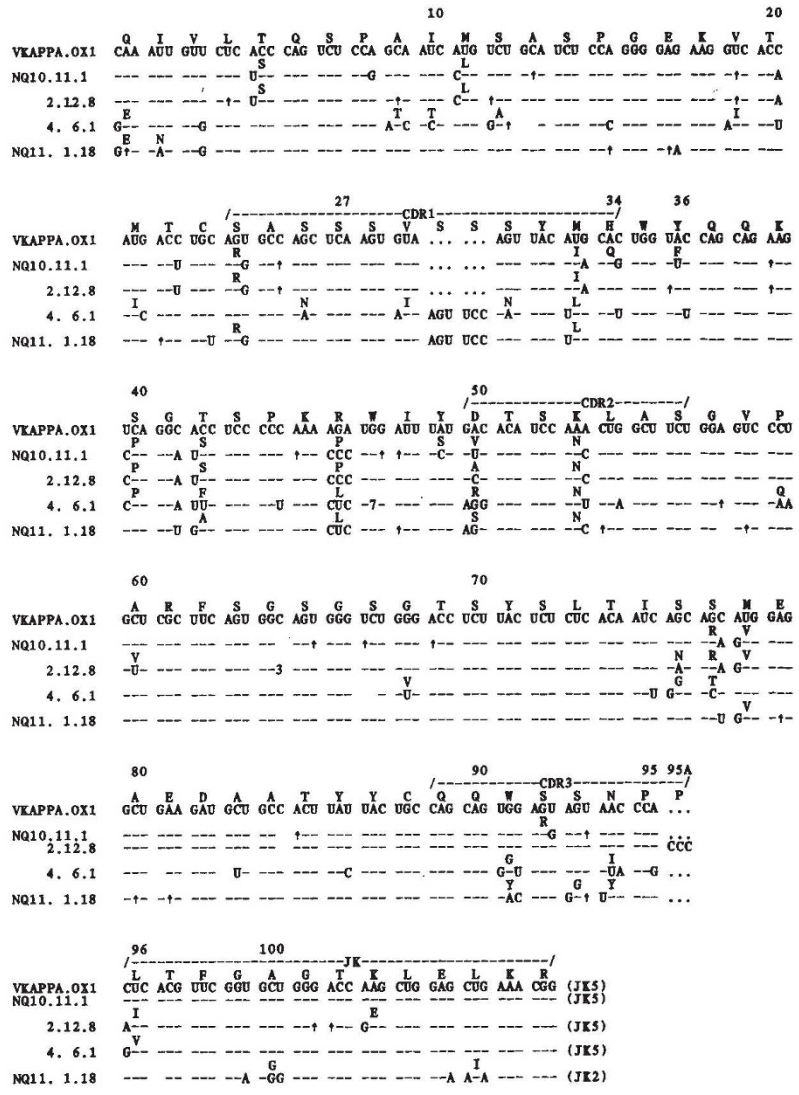

Fig. 1 Immunoglobulin light-chain mRNA sequences for secondary hybridoma lines with specificity for phenyloxazolone: V_κ-Ox1-related sequences. The top line shows the nucleotide sequence of the germline gene *V_κ-Ox1* joined to the *J_κ5* gene segment (ref. 15 and J. Even, unpublished results). The amino-acid translation is shown above, with numbering according to Kabat[22]. The complementarity-determining regions (CDR1, 2, 3) and the *J* segment are indicated. The V_κ sequences of the different hybridoma lines are given beneath. Dashes indicate identity with the top line, an arrow marks probable identity, a gap that the nucleotide could not be identified. A computer code is used to denote sequence ambiguities[23]: 1, probably C; 2, probably T; 3, probably A; 4, probably G; 5, A or C; 6, G or T; 7, A or T. Established nucleotide differences and the predicted amino-acid changes are indicated.

Methods. Mice were immunized intraperitoneally with 30 μg alum-precipitated phOx coupled to the carrier chicken serum albumin (phOx-CSA)[21] and 6 weeks (fusion NQ10) or 8 weeks (fusion NQ11) later boosted with an intravenous injection of 100 μg phOx-CSA. Three days later, spleen cells of individual mice were fused with the non-secretor line NSO and hybridoma lines screened for secretion of phOx-specific antibodies. Isolation and sequencing of the mRNA were done as described previously[11,24].

Secondary response to oxazolone

Hybridomas of the secondary response were prepared from mice boosted 6 weeks (fusion NQ10) or 8 weeks (fusion NQ11) after primary immunization with phOx coupled to chicken serum albumin (phOx-CSA)(see Fig. 1 legend). In both experiments there was a strong secondary response yielding ~30% of hybridomas specific for the hapten phOx. Several of these lines were randomly taken, cloned and the mRNA of the H and the L chain sequenced.

In the secondary response, only 4 out of the 23 lines were related to the *V_κ-Ox1* with *V_H-Ox1* combination[11], indicating a shift to new germline H/L-chain combinations (Table 1). The expression of H chains was more complex than L chains and V_H subgroups emerged which had not been detected at earlier stages of the response (Table 1). For this reason we will analyse the data classified by the criteria of L-chain subgroups.

V_κ-Ox subgroup antibodies

Most of the L chains of the V_κ-Ox subgroup are derived from a single germline gene, *V_κ-Ox1*[10,11]. Sequences closely related to *V_κ-Ox1* but probably derived from other germline genes were also detected throughout the response (Table 1). These are the L chains of NQ2/6.1 and NQ2/45.10.4 from day 7 (ref. 10) and NQ10/11.1, NQ10/2.12.8, NQ10/4.6.1 and NQ11.18 from the secondary response (Fig. 1). These L chains show an 85–95% homology with the Ox1 prototype sequence. We believe that these V_κ segments originate from different germline genes. Compared with *V_κ-Ox1*, NQ11/1.18 and NQ10/4.6.1 (originating from different mice) have an identical insertion of six extra residues in the first complementarity-determining region (CDR1). Furthermore, NQ10/2.12.8 and NQ10/11.1 show the same residue at 15 positions which differ from the prototype *V_κ-Ox1* sequence. Although these two lines originate from the same mouse, they are independent cell lines because the L chains are combined with very different H chains (Fig. 2).

In the secondary response, L chains of the V_κ Ox subgroup are often associated with V_H segments which have not been observed in the primary response (Table 1). These V_H sequences differ considerably from those encoded by *V_H-Ox1*. The homology is 70% at the nucleotide level and only 60% at the translated amino-acid level. Four of them (NQ10/12.5, NQ10/11.1, NQ10/15.3 and NQ11/8.1) belong to the V_H group 5 (MOPC21 gene family)[12,13], NQ11/7.12 and NQ11/1.18 to the V_H group 1 (J558 gene family), and NQ10/2.12.8 and NQ10/4.6.1 to the V_H group 3 (germline gene V_H-1210.7)[14] (Fig. 2). V_H regions encoded by the MOPC21 or J558 gene family are one amino acid longer in CDR2 (residue 52A) than V_H-Ox1.

Other V_κ subgroups

Two of the day 7 hybridomas did not express L chains of the V_κ-Ox subgroup. The L chain of one of them (NQ2/45.1) was also found in the day 14 hybridoma NQ7/47.1, and in 10 out of 23 of the secondary response hybridomas (Table 1). Most of the sequences appear identical to *V_κ-45.1* (Fig. 3) except for the pair NQ10/2.22 and NQ10/12.22, which differed at three positions from the *V_κ-45.1* prototype sequence, as well as NQ10/2.12.4, an IgM hybridoma which has one substitution at the third base of triplet 34. The last base of the *V_κ*-region

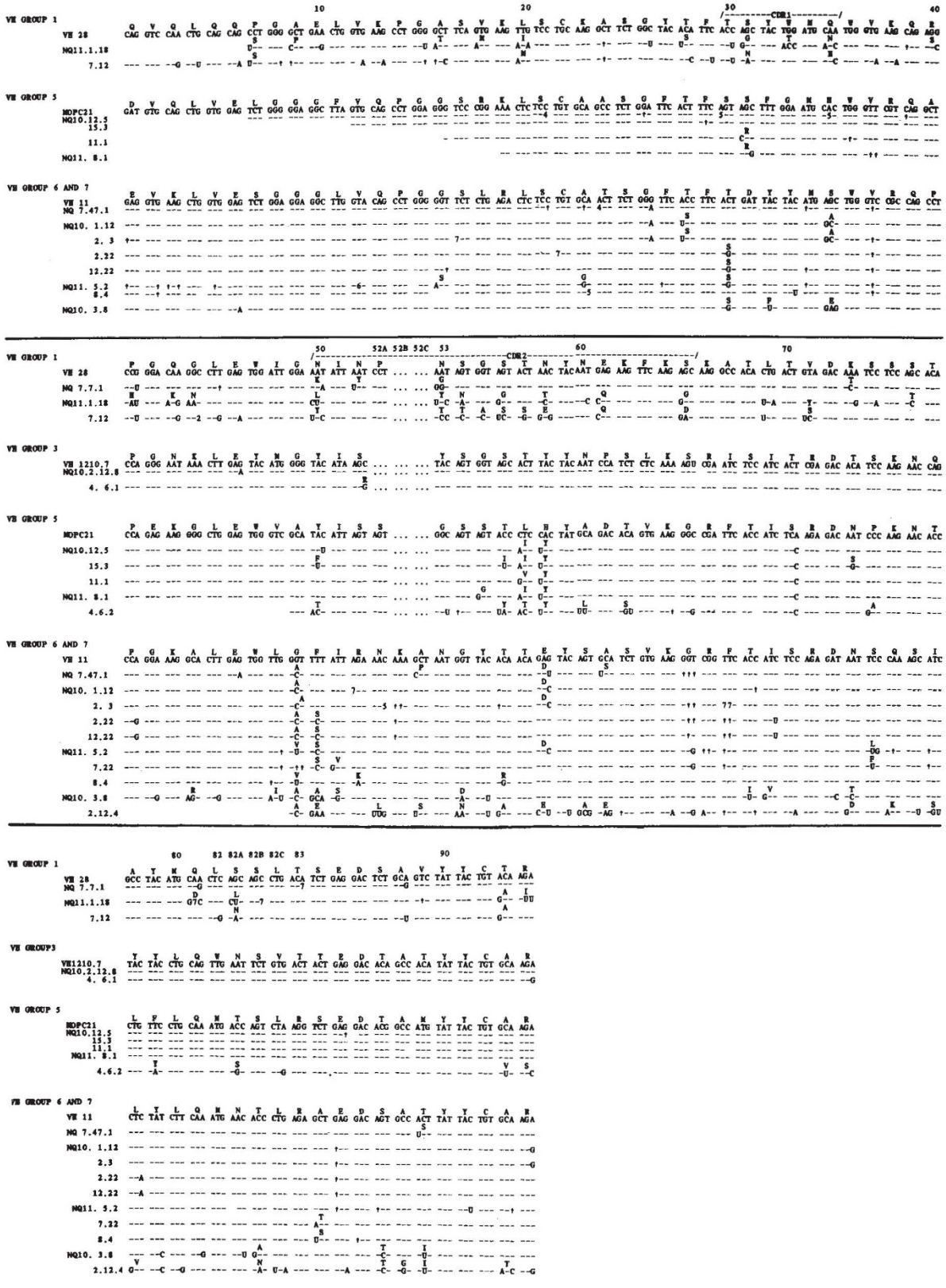

Fig. 2 Immunoglobulin H-chain mRNA sequences: V segments from anti-phenyloxazolone hybridomas. V_H regions characteristic of five different V_H-gene families were found: the H-chain mRNA sequences of the hybridoma lines NQ10/11.1, NQ10/12.5, NQ10/15.3, NQ11/8.1 and NQ10/4.6.2 are compared with the V_H region of the myeloma line MOPC21 (V_H group 5)[25], those of the hybridoma lines NQ7/7.1, NQ11/1.18 and NQ11/7.12 with the germline gene *V_H-28* (V_H group 1)[26], those of the hybridoma lines NQ10/2.12.8 and NQ10/4.6.1 with the germline sequence *V_H-1210.7* (V_H group 3)[14] and the mRNA sequences of the hybridoma lines NQ7/47.1, NQ10/1.12, NQ10/2.3, NQ10/2.22, NQ10.12.22, NQ11/5.2, NQ11/7.22, NQ11/8.4 (V_H group 7) and NQ10/1.12.4 (V_H group 6) are compared with the germline sequence *V11* (ref. 16). For mRNA sequencing, primers C_μ-15 and C_γ-15 have been described previously[10]; to complete MOPC21-related V_H regions, a V_{M21}-14 d(TGGTAGAGGTCTCT), which primes between amino acids 68 and 72, was used. To determine V_H regions of the J558 gene family, a V_H2-15 d(TCGGACTGTAGACTC) primer complementary to the sequence between residues 82B and 85 was used. For sequences of the V_H group 7, two primers, V_{M21}-14 and V_{T15}-14 (ref. 27), were used. Fur further details see Fig. 1 legend.

Table 1 V_κ/V_H combinations found in phenyloxazolone-specific hybridoma lines

V_H (according to ref. 12)	V_κ-Ox: Ox1	V_κ-Ox: Other	V_κ-*ars*	V_κ-*45.1*
Group 2 (V_H-Ox1)	NQ10/ 2.2.5 (γ1)* 12.4.6 (γ1) 15.9 (γ1) NQ11/14.5 (μ)	NQ2 /45.10.4(μ)†	NQ5 /89.4 (γ1)† NQ10/12.4.7 (γ1)	
Group 1 J558)	NQ11/7.12 (γ1)	NQ2 /6.1 (γ1)† NQ11/1.18 (γ1)	NQ7 /7.1 (μ)†	NQ2 /45.1 (γ1)†
Group 3		NQ10/2.12.8 (μ) /4.6.1 (γ1)		
Group 5 (MOPC21)	NQ10/12.5 (γ1) 15.3 (γ1) NQ11/ 8.1 (γ1)	NQ10/11.1 (γ1)		NQ10/4.6.2 (γ1)
Group 6 (J606)				NQ10/2.12.4 (μ)
Group 7 (TEPC15)				NQ7 /47.1 (γ1)† NQ10/ 1.12 (γ1) 2.3 (γ1) 2.22 (γ1) 3.8 (μ) 12.22 (γ1) NQ11/ 5.2 (γ2a) 7.22 (γ1) 8.4 (μ)

* This block refers to 11 hybridomas from day 7, and 8 from day 14 response having the V_HOx–V_κ-4Ox1 combination[10,11,21].

† Hybridoma lines NQ2 and NQ5 are derived from the day 7, and hybridoma lines NQ7 from the day 14 response. Their sequences are either published elsewhere[10,11,21] or presented in Figs 1–5. Immunoglobulin classes of the hybridoma lines are shown.

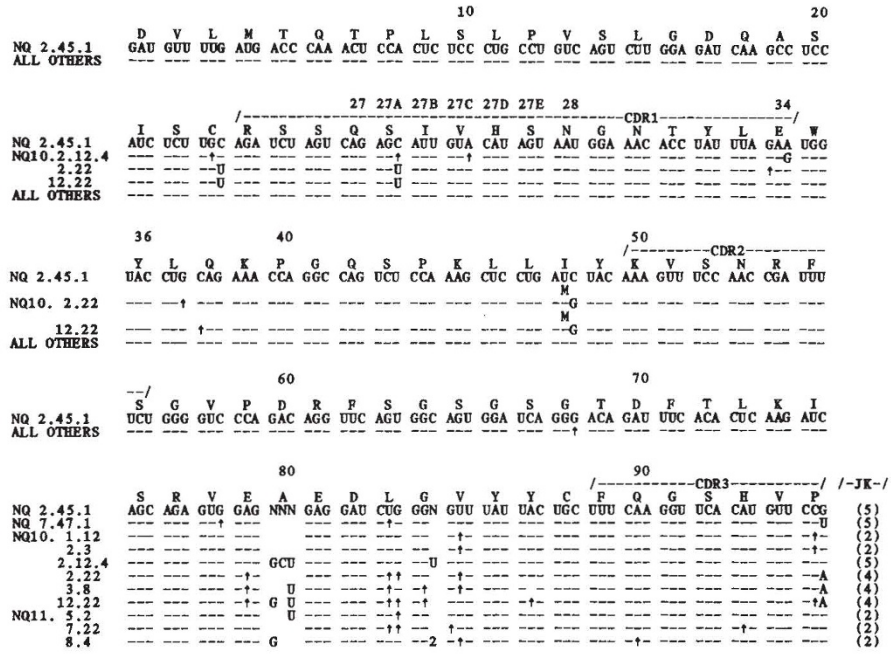

Fig. 3 L-chain mRNA sequences related to the sequence of the day 7 hybridoma line NQ2/45.1. The top row shows the corrected sequence of the hybridoma line NQ2/45.1 (ref. 10). By using alternative primers some of these sequences could be completed:

J_κ2-15 d(GACCTTTATTTTGCC)

or

J_κ4-15 d(AACCTTTATTTTGCC),

which prime between residues 104 and 108 of the rearranged J_κ segments. For further details see Fig. 1 legend.

differences could be the result of junctional diversity. Thus, the A residue could originate from germline J_κ4 and the G from J_κ5 or J_κ2 (ref. 15). The U of NQ7/47.1 cannot originate from the J_κ gene so is either from the V_κ-*45.1* germline gene or a somatic variant.

Among the anti-phOx hybridomas there was a marked association of the expression of the V_κ-*45.1*-encoded L chain with H chains related to V_H regions encoded in the T15 gene family (V_H group 7). Four germline genes have been described for this family and named *V1*, *V3*, *V11* and *V13* (ref. 16). The V_H sequence of NQ10/3.8 was identical to the sequence of the *V1* germline gene (Fig. 2). The mRNA sequences of NQ10/2.22, NQ10/12.22, NQ10/1.12, NQ10/2.3, NQ11/5.2, NQ11/7.22 and NQ11/8.4, as well as the day 14 hybridoma NQ7/47.1, were most closely related to the *V11* germline gene, but differed by 5–10 nucleotides (Fig. 2). Although these differences could result from somatic mutation, a comparison of these V_H sequences with other genes of the T15 gene family suggests that there are more, as yet undescribed, germline genes in this family.

Two other H chains were found in association with V_κ-45.1 (Fig. 2): one, NQ10/2.12.4, has a V_H region belonging to V_H group 6 (J606 gene family); the other, NQ10/4.6.2, has a V_H region very similar to the sequences of the MOPC21 gene family.

The L chain of the secondary response hybridoma NQ10/12.4.7, although derived from a BALB/c mouse, is very similar to the L chains found in arsonate-specific antibodies of the A/J mouse. This L chain, which is only 65% homologous with V_κ-Ox1, has also been found in the day 7 (NQ5/89.4) and

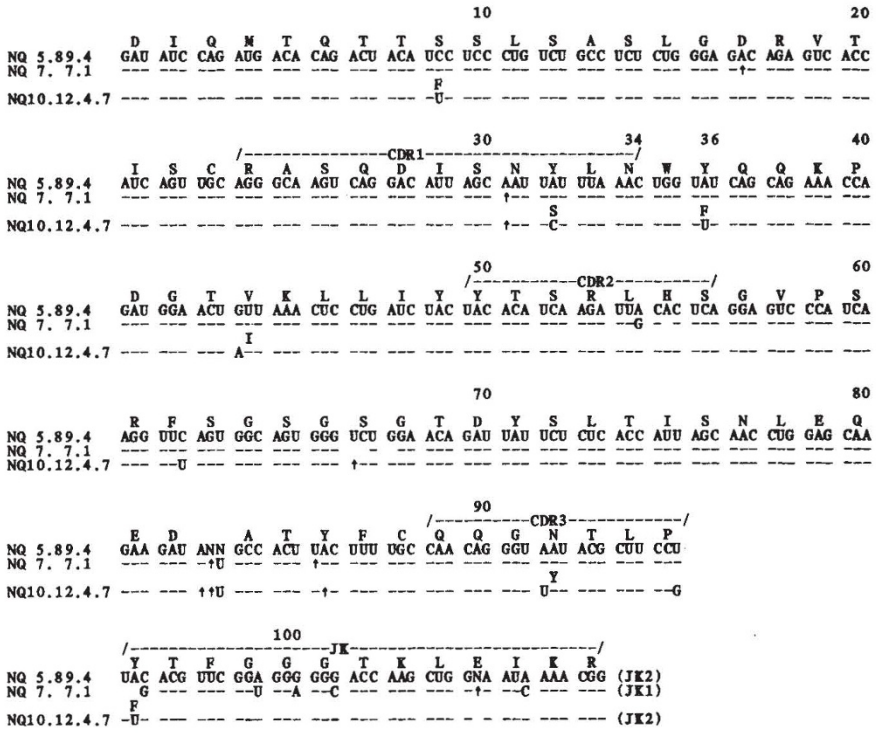

Fig. 4 L-chain mRNA sequences related to V_κ-*ars*. Sequences are compared with the L-chain sequence of the day 7 hybridoma line NQ5/89.4 (ref. 10). For further details see Fig. 1 legend.

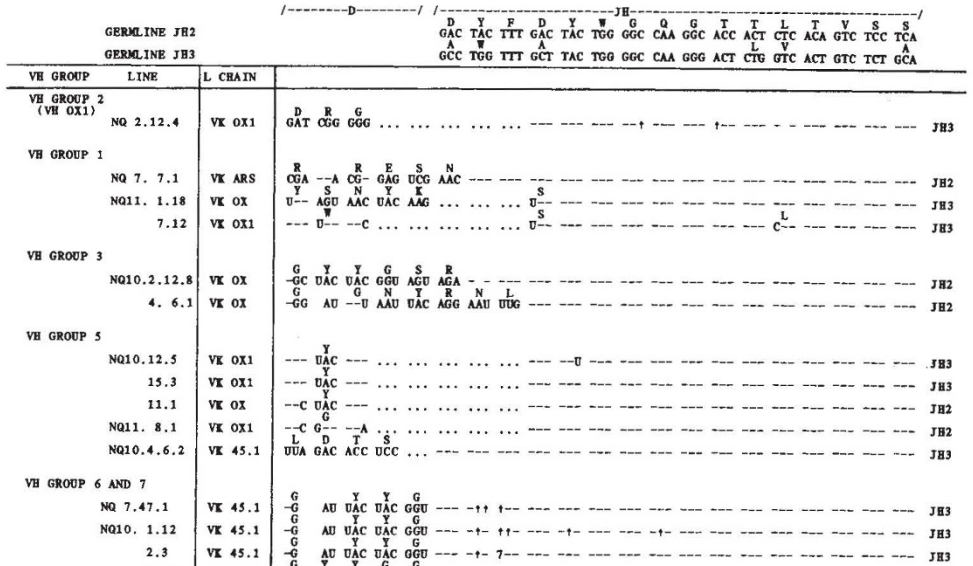

Fig. 5 *D–J* region of H-chain mRNA from anti-phenyloxazolone-specific hybridoma lines. *D–J* regions of the H-chain mRNA sequences in Fig. 2 are shown. L chains found in association with these H chains are given. *D* regions are compared with the D segment of hybridoma NQ2/12.4, characteristic for primary-response Ox1 antibodies[10]. The J_H regions are either J_H2 or J_H3 (respective germline sequences[28] are shown in the top line). The length of the *J* segment is indicated by dashes.

day 14 (NQ/7.1) hybridomas (Fig. 4). The differences between the V_κ-arsonate (*ars*) L-chain mRNA sequences of the hybridoma lines obtained at different stages of the immune response to phOx are consistent with somatic mutants of a single V_κ-*ars* germline gene (Fig. 4). In NQ5/89.4 and NQ10/12.4.7 V_κ-ars L chains combine with an Ox1 H chain[10,11] while NQ7/7.1 has a V_H region related to sequences of the J558 gene family (Fig. 2).

D–J segment and light-chain type

The V_H regions of all anti-phOx antibodies that use V_κ-Ox1 have a characteristic D segment, although the V_H regions belong to different V_H-gene families, V_H-*Ox*, V_H-*MOPC21* or V_H-*J558*. In all cases the D segments are three amino-acid residues long (Fig. 5). The first triplet is either a GAU or GAC, both encoding Asp. The third triplet, encoding Gly, again shows variability in codon usage. Diversity expressed at the protein level was found only for the middle residue of the D segment. H chains combining with V_κ-Ox1 have another feature in common, which is not shared with H chains associated with other L chains, namely the length of CDR3 and fourth framework region (FR4) (Fig. 1 and refs 10, 11). In all these cases the J_H segment is shorter than its germline counterpart. This is even more noteworthy as different J_H segments are used: J_H2, J_H3 and J_H4 (Fig. 5 and refs 10, 11).

The H chains of NQ10/2.12.8, NQ10/4.6.1 and NQ11/1.18 (but not NQ10/11.1; Fig. 5) have longer D segments but these H chains are combined with V_κ-Ox L chains which differ from V_κ-Ox1 in important aspects. NQ10/4.6.1 and NQ11/1.18 are two triplets longer in the CDR1 and NQ10/2.12.8 one triplet longer in the CDR3 than the V_κ-Ox1 L chain (Fig. 2).

Hybridomas expressing a V_κ-*45.1* L chain again have closely

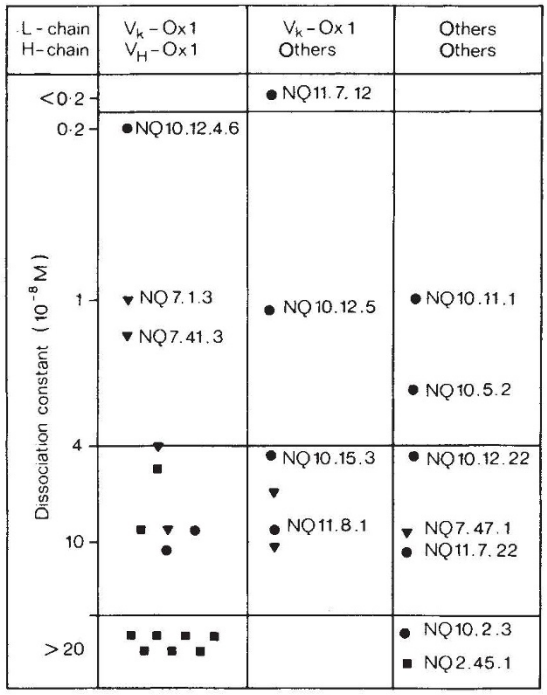

Fig. 6 Dissociation constants of phOx-specific hybridoma proteins. Dissociation constants of hybridoma lines obtained at three different stages of the immune response to phOx (day 7 (■), day 14 (▼), primary and secondary (●) response) are shown. Data are plotted according to the V_H/V_κ combination of the antibody molecules. Symbols with no designation show results from hybridoma lines described previously[10,11]. Affinity measurements were performed by the method of fluorescence quenching with the hapten phOx-cap[29]. Antibodies with affinities $<4\times10^{-8}$ M were further analysed by the method of equilibrium dialysis, using ^{3}HphOx-aminobutyrate.

related D-J region sequences. In 9 out of 12 the V_H region is followed by D segments 5 amino-acid residues long (Fig. 5 and ref. 9). These include hybridomas of three independent fusions and one (NQ10/2.12.4) expressing a H chain of a different V_H-gene family. All these have a J_H3 segment of 16 residues. As discussed above, the strong correlation of the length of CDR3/FR4 in H chains of antibodies of a given specificity points to the importance of the interaction between this region and the L chains for the structure of the antibody-combining site.

Affinity maturation

To measure the affinity of the anti-phOx antibodies, we have used the method of fluorescence quenching[17] by 2-phenyl-5-oxazolone aminocaproyl (phOx-cap) (Fig. 6). This method becomes inaccurate for affinities approaching 10^{-8} M. To determine affinities below 4×10^{-8} M more accurately, we used equilibrium dialysis. Antibodies of the early primary response had dissociation constants of $\sim3\times10^{-7}$ M. In only one example was it significantly below 10^{-7} M (ref. 10). During the late primary response almost all of the antibodies had dissociation constants well below 10^{-7} M (ref. 11). In the secondary response, some of the antibodies showed a further increase in affinity. Antibodies NQ10/12.4.6 (V_κ-Ox1-V_H-Ox1) and NQ11/7.12 (V_κ-Ox1-V_H group 1) were at least fivefold better than the two best of the day 14 response. What we find remarkable is that despite the increased number of somatic mutations[11], only one out of three secondary-response Ox1 antibodies had affinity constants below 4×10^{-8} M (Fig. 6). On the other hand, three out of four secondary-response antibodies expressing V_κ-Ox1 in combination with a H chain other than V_H-Ox1, had similar high affinity.

Taken together, these results suggest that further point mutations of the V_H-Ox1-V_κ-Ox1 combination did not necessarily lead to an improvement in the affinity of the hapten beyond that achieved at day 14. Other germline combinations were a fresh source for such improvements.

Diversity and response maturation

Three stages of the maturation of the antibody response to oxazolone have been studied. Each stage involved the sequence analysis of the L- and H-chain mRNA of between 11 and 23 hybridomas. In the first stage (7 days after primary immunization) the hybridomas reflect the selection of a germline gene rearrangement which happens to display good affinity. In the second stage (14 days after primary immunization) the antibodies expressing the unmutated germline genes characteristic of day 7 disappear and are largely replaced by drift of the same germline genes, modified by point mutations in all segments of the *V* regions including the *J* segments. The point mutations tend to accumulate at certain positions (for example, residues 34 and 36 of V_κ-Ox1) even in hybridomas of different clonal origin, suggesting mutational hotspots and/or a strong selective pressure to accommodate hitherto unknown interactions with ligands, probably antigen itself. Although mutant forms of the *V_H-Ox1-V_κ-Ox1* combination constitute most of the late primary-response hybridomas, a shift to alternative germline combinations begins to become apparent. This shift is the dominant feature of the secondary-response hybridomas. At this third stage, only a few hybridomas express the *V_H-Ox1-V_κ-Ox1* combination and these show further mutational drift. These additional mutations do not always correlate with an increase in affinity for the hapten. The *V_κ-Ox1-V_H-Ox1* combination, although useful to start with, may become increasingly difficult to mutate towards further improvement of binding. On the other hand, other germline gene combinations may be a better starting point from which high-affinity antibodies can be produced following a few key mutations.

The question arises of why these combinations, which are only rarely seen in late primary responses (for example, V_H group 7 and V_κ-45.1), become dominant in the secondary. A calculation can help to clarify the problem. If we assume a total of 200 *V* genes and 4 *J* segments for each chain and 20 *D* gene segments, random assortment results in 800 κ and 16,000 H chains. In addition, there is junctional diversity, which increases by at least a factor of 2.5 the number of possible κ chains to 2,000. As for the H chain, the same factor of 2.5 for junctional diversity is applicable to *V/D* and *D/J* boundaries. Considering variations in the length for both *J* and *D* segments[10], an additional factor of 5 is an underestimate. Without bringing into the calculation the potential diversity generated by the postulated *N* regions[18], this takes the total of potential H-chain V regions, quite apart from somatic variants, to 500,000. The combinatorial association of κ and H chains gives a total of 10^9, more than the total number of lymphocytes in a mouse. Although the combinatorial expression is unlikely to be random[19] and not all junctional or combinatorial diversity will be structurally viable, it is possible that the mouse does not express at any given moment all the variants which it can potentially generate by using the unmutated germline genes. It follows that the first expression of the response will be dominated by the frequency at which certain combinations occur as much as by the affinity for the antigen. The expression of a low-frequency germline gene combination of an infrequent joining variant, or even a random favourable point mutation, could eventually arise and start the shift to a new germline set. Persistence of antigen expands these rare cells into a proliferating population from which mutants can be selected. A shift to new germline gene combinations may have as a secondary effect an increase in potential cross-reactive antibodies. This could explain the apparent paradox of an increase in the cross-reactivity of the antiserum of a secondary response[20] while the monoclonal antibodies derived from it have increased affinity (that is, specificity) for the immunogen.

In summary, we suggest that the initial selection of germline gene combinations is based both on frequency and affinity. This is followed by two events. One, selection of somatic mutants of the initial proliferating dominant clones expressing those genes, and second, the active recruitment of other germline gene

combinations. Among these new germline gene combinations, those having the best potential to be modified by somatic mutation into more suitable combining sites will give rise to the very high-affinity antibodies that characterize the mature response. Our experiments do not allow us to say whether the shift to other germline genes is selected by antigen alone or whether there is some other mechanism which favours that shift, such as anti-idiotypic suppression of the initial idiotype, separate compartmentalization of memory and virgin B cells or senescence of early-stimulated clones.

We thank Mr J. Jarvis for measuring the affinity of the antibody molecules, Dr M. Waye for preparation of oligonucleotide primers, Dr R. Staden for the computer analysis, Dr M. Kaartinen for gifts of oxazolone derivatives, Dr M. Neuberger for helpful discussions, and Miss J. Firth for preparation of the manuscript.

Received 18 March; accepted 13 June 1985.

1. Siskind, G. W. & Benaceraff, B. *Adv. Immun.* **10**, 1-50 (1969).
2. Cosenza, H. & Köhler, H. *Proc. natn. Acad. Sci. U.S.A.* **69**, 2701-2705 (1972).
3. Nisonoff, A., Ju, S. T. & Owen, F. L. *Immun. Rev.* **34**, 89-118 (1977).
4. Jack, R. S., Imanishi-Kari, T. & Rajewsky, K. *Eur. J. Immun.* **7**, 559-565 (1977).
5. Mäkelä, O. & Karjalainen, K. *Transplantn Rev.* **34**, 119-138 (1977).
6. Reth, M., Hämmerling, G. J. & Rajewsky, K. *Eur. J. Immun.* **8**, 393-400 (1978).
7. Chang, S. P., Brown, M. K. & Rittenberg, M. B. *J. Immun.* **128**, 702-706 (1982).
8. Chang, S. P. *et al. J. Immun.* **132**, 1550-1555 (1984).
9. Tonegawa, S. *Nature* **302**, 575-581 (1983).
10. Kaartinen, M., Griffiths, G. M., Markham, A. F. & Milstein, C. *Nature* **304**, 320-324 (1983).
11. Griffiths, G. M., Berek, C., Kaartinen, M. & Milstein, C. *Nature* **312**, 271-275 (1984).
12. Dildrop, R. *Immun. Today* **5**, 100-101 (1984).
13. Brodeur, P. H. & Riblet, R. *Eur. J. Immun.* **14**, 922-930 (1984).
14. Near, R. J. *et al. Proc. natn. Acad. Sci. U.S.A.* **81**, 2167-2171 (1984).
15. Sakano, H., Hüppi, K., Heinrich, G. & Tonegawa, S. *Nature* **280**, 288-299 (1979).
16. Crews, S., Griffin, J., Huang, H., Calame, K. & Hood, L. *Cell* **25**, 59-66 (1981).
17. Parker, C. W. *Handbook of Experimental Immunology* 3rd edn, Ch. 18 (Blackwell Scientific, Oxford, 1978).
18. Alt, F. W. & Baltimore, D. *Proc. natn. Acad. Sci. U.S.A.* **79**, 4118-4122 (1982).
19. Yancopoulos, G. D. *et al. Nature* **311**, 727-733 (1984).
20. Sperling, R., Francus, T. & Siskind, G. W. *J. Immun.* **131**, 882-885 (1983).
21. Kaartinen, M. *et al. J. Immun.* **130**, 937-945 (1983).
22. Kabat, E. A. *et al. Sequences of Proteins of Immunological Interest* (NIH, Bethesda, 1983).
23. Staden, R. *Nucleic Acids Res.* **10**, 4731 (1982).
24. Griffiths, G. M. & Milstein, C. in *Hybridoma Technology in the Biosciences and Medicine* (ed. Springer, T. A.) (Plenum, New York, in the press).
25. Bothwell, A. L. M. *et al. Cell* **23**, 625-637 (1981).
26. Loh, D. Y., Bothwell, A. L. M., White-Scharff, M. E., Imanishi-Kari, T. & Baltimore, D. *Cell* **33**, 85-93 (1983).
27. Berek, C. *Eur. J. Immun.* **14**, 1043-1048 (1984).
28. Sakano, H., Maki, R., Kurosawa, Y., Roeder, W. & Tonegawa, S. *Nature* **286**, 676-683 (1980).
29. Makela, O., Kaartinen, M., Pelkonen, J. L. & Karjalainen, K. *J. exp. Med.* **148**, 1644-1660 (1978).

LETTERS TO NATURE

Anatomy of a cosmic-ray neutrino source and the Cygnus X-3 system

F. W. Stecker, A. K. Harding & J. J. Barnard

Laboratory for High Energy Astrophysics, NASA/Goddard Space Flight Center, Greenbelt, Maryland 20771, USA

There is strong evidence that a compact object in the Cygnus X-3 binary system produces an intense beam of ultra-high-energy cosmic rays. Here, we examine the effects of such a beam hitting the companion star and of the subsequent production of secondary neutrinos. We consider how high a beam luminosity is allowed and how high a neutrino to γ-ray (ν/γ) ratio can be obtained from such a system. We find a maximum allowable beam luminosity of $\sim 10^{42}$ erg s^{-1} for a system consisting of a compact object and a $\sim$ 1–10 $M_\odot$ main-sequence target star. The proton beam must heat a relatively small area of the target star to satisfy observational constraints on the resulting stellar wind. With such a model, a ν/γ flux ratio of $\sim 10^3$ can result from a combination of γ-ray absorption and a large ν/γ duty cycle ratio. We find that the high density of the atmosphere resulting from compression by the beam leads to pion cascading and a neutrino spectrum peaking at 1–10 GeV energies, which may avoid catastrophic heating of the target star through internal ν interactions. The ν flux and duty cycle are predicted to be accordingly reduced in the energy range above 1 TeV available to a deep underwater neutrino detector.

There has recently been much interest in constructing theoretical models for the Cyg X-3 binary system[1-3] in view of the discovery of ultra-high-energy γ rays from this source[4-6]. The γ-ray flux implies that Cyg X-3 is the first identified source of ultra-high-energy cosmic rays and that the source power is at least 10^{39} erg s^{-1} in cosmic-ray primaries, enough to provide a significant fraction of the 10^{17}-eV cosmic rays in the Galaxy[7]. It has been suggested that Cyg X-3 may be a source of cosmic-ray neutrinos[8,9], produced from the pion decay processes[10] which probably produce the γ rays. This possibility has taken on more interest with the detection of muon signals in deep underground proton decay detectors (ref. 11 and J. Learned, personal communication) from the direction of Cyg X-3 with the 4.8-h periodicity of the Cyg X-3 system. (Such detectors make use of the Cerenkov light emitted by charged particles crossing large volumes of water[12].) The very detectability of such signals, if induced by cosmic-ray neutrinos from Cyg X-3, implies a surprisingly large neutrino flux, primary cosmic-ray beam power ($\gg 10^{39}$ erg s^{-1}) and neutrino-to-γ-ray flux ratio. In the event that the recently detected muons are produced by some other 'X' particle, a large beam power and accompanying neutrino flux are almost certainly implied. Therefore, regardless of the outcome of the present observational situation, it is of interest to consider the theoretical implications of significantly larger beam power.

Hillas[2] has recently presented calculations of γ-ray production from an energetic proton beam, based on a model originally proposed by Vestrand and Eichler[13]. In this model, a beam of $\sim 10^{17}$ eV protons, accelerated at a compact object, impinges on the atmosphere of a companion star, initiating a cascade producing γ rays below 10^{16} eV. The total luminosity of the compact source required to account for the observed γ rays above 10^{12} eV is $L_T = 6.4\times10^{39}\,(\varepsilon_\gamma/0.1)^{-1}(\langle\Omega_B\rangle/4\pi)(0.025/\Delta\gamma)$ erg s^{-1}, where $\langle\Omega_B\rangle$ is the time-averaged solid angle of the proton beam, ε_γ is the fraction of proton energy converted into γ rays and Δ_γ is the duty cycle of the pulse $\sim$0.025 (ref. 5). Owing to observational uncertainty, a smaller Δ_γ cannot be ruled out, which would imply an even larger beam luminosity. If the part of the beam luminosity striking the target star, L_B, is greater than its Eddington limit,

$$L_{edd} = \frac{4\pi GcM_*}{\kappa} = 1.3\times10^{38}\,\tilde{M}\ \text{erg s}^{-1} \qquad (1)$$

where M_* is the target star mass and κ is the electron scattering opacity, a mass loss will result. (Note that all quantities with overbars will be in solar units, for example, $\tilde{R} = R/R_\odot$). The mass loss from the system is limited by the observed derivative, $\dot{P}$, of the 4.8-h orbital period[14], through the relation[15]

$$\dot{P}/P = 2\dot{M}/M_T \qquad (2)$$

where M_T is the total mass of the system and $\dot{M}$ is the mass loss rate from the target star (assuming that the orbital angular momentum is lost from the system and that the orbit decay from gravitational radiation is small). When the beam hits the atmosphere of the target star, roughly half of the beam energy flux will be thermalized in the stellar atmosphere, producing an outward radiative flux. The resulting radiation pressure can drive a wind with a terminal velocity v given by

$$v^2 = \frac{2}{R_*}\left(\frac{L_B\kappa}{4\pi fc} - GM_*\right) \qquad (3)$$

where R_* is the target star radius and f is the fraction of the